Catalysis Today 168 (2011) 48–56

Contents lists available at ScienceDirect

Catalysis Today

journal homepage: www.elsevier.com/locate/cattod

Alkaline treatment of template containing zeolites: Introducing mesoporosity while preserving acidity

Adri N.C. van laak, Lei Zhang, Andrei N. Parvulescu, Pieter C.A. Bruijnincx, Bert M. Weckhuysen, Krijn P. de Jong, Petra E. de Jongh*

Inorganic Chemistry and Catalysis, Debye Institute for Nanomaterials Science, Utrecht University, Sorbonnelann 16, Utrecht, Netherlands

ARTICLE INFO

Article history:
Received 18 August 2010
Received in revised form 24 October 2010
Accepted 26 October 2010
Available online 6 January 2011

Keywords:
Template
Zeolites
Mesoporosity
Desilication
Catalysis

ABSTRACT

Alkaline treatment (desilication) is an effective treatment to increase mesoporosity. However, the concomitant decrease in Si/Al ratio affects the strengths of the acidic sites and hence catalytic activity and selectivity. Therefore instead we subjected *template containing* zeolites to 1 M NaOH to induce additional porosity. All zeolites tested (ZSM-5, ZSM-12 and Beta) consisted of small crystallites (30–200 nm) that were agglomerated into larger particles between 1 and 5 μm. Mesopore formation occurred by slowly removing outer layers of individual crystallites, thereby preserving the Si/Al ratio as well as the crystallinity. Inter-crystalline mesopores were formed for all zeolites, but the treatment was most effective for zeolites with small crystallites. The external surface area of ZSM-5 was increased from 90 to 149 $m^2\ g^{-1}$ and for zeolite Beta from 70 to 158 $m^2\ g^{-1}$. The catalytic performance was tested at 413 K for 3 h for etherification of 1,2-propylene glycol with 1-octene to form octyl-ether. For ZSM-5, conversion increased from 1.2% to 5.6% upon alkaline treatment in the presence of a template, while only to 5% for the template-free treated sample with a significantly higher external surface area (205 $m^2\ g^{-1}$). The parent zeolite Beta was significantly more active (30% conversion, 88% selectivity), which can be ascribed to its larger pore size. Nevertheless also in this case alkaline treatment in the presence of the template significantly increased the activity to 40% conversion with similar selectivity. As only the mesoporosity was changed upon alkaline treatment it suggests that the etherification of 1,2-propylene glycol with 1-octene is affected by intra-crystalline diffusion. Our work illustrates the possibilities to use alkaline treatment of templated zeolites to decouple accessibility changes from acidity, and to gain further insight in zeolite catalysis.

1. Introduction

Zeolites are microporous crystalline aluminosilicates that represent an important class of catalysts in the petrochemical industry. Finding new and improved synthesis routes has been essential to the success of zeolites. An important development in zeolite synthesis was the use of organic molecules, such as the tetramethylammonium (TMA) halide or hydroxide, that can facilitate the synthesis of known and new zeolites [1–4]. Nowadays these structure directing agents, such as alkyl-ammonium hydroxides and amines, have greatly contributed to the content of the Atlas of Zeolites [5] that contains over 190 structures.

Post-synthesis treatments, such as steaming and acid-leaching, are important to induce mesoporosity and further enhance the catalytic performance of zeolites, especially in diffusion limited reactions [6]. Recently also alkaline treatment (desilication) was explored as a post-synthesis tool to increase the porosity, and thereby the activity, of zeolites [7,8]. The desilication process was further improved by Groen et al. [9,10] who determined that the best results for ZSM-5 are obtained with 0.2 M NaOH for 30 min at 328 K with a Si/Al ratio between 25 and 50 at/at. At lower values the aluminum prevents desilication, thereby limiting mesopore formation, while at higher values complete dissolution occurs. It was also observed that alkaline treatment can affect tetrahedrally coordinated aluminum, resulting in loss of acidic properties of zeolite Beta [11] thereby decreasing the catalytic activity. Recently Holm et al. [12] showed that desilication of ZSM-5 zeolite results in the formation of strong Lewis sites most likely as a result from extra framework aluminum. Groen et al. [13] and Fernandez et al. [14] showed that desilication leads to redistribution of aluminum and enrichment of aluminum at the external surface and near the pore mouths.

Several studies show that templates can be helpful for successful alkaline treatment. Pérez-Ramírez et al. reported that partial detemplation followed by alkaline treatment [15] can be used to tune the desilication process and that the addition of template molecules (TPA^+ or TBA^+) during desilication can be used as pore growth moderators [16]. Holm et al. showed that a TMA-hydroxide solution can

* Corresponding author. Tel.: +31 30 253 7400; fax: +31 30 251 1027.
E-mail address: p.e.dejongh@uu.nl (P.E. de Jongh).

0920-5861/$ – see front matter © 2010 Elsevier B.V. All rights reserved.
doi:10.1016/j.cattod.2010.10.101

be used to obtain mesoporous zeolite Beta [17]. A study by Wei and Smirniotis [18] showed that templated ZSM-12 samples with Si/Al ratio up to 500 (at/at) were protected from silicon extraction during alkaline treatment.

In this study alkaline treatment on template containing zeolites with industrial importance, such as ZSM-5, ZSM-12 and zeolite Beta, is discussed. It is shown that alkaline treatment on templated zeolites can be used to increase the porosity without changing the crystallinity or acidity of the zeolites regardless of the framework type and Si/Al ratio. This enables the decoupling of accessibility and acidity, and can be used to improve the scope as well as the understanding of zeolite catalyzed reactions.

2. Experimental

2.1. Zeolite synthesis

ZSM-5 was synthesized at the laboratories of ExxonMobil European Technology (Machelen, Belgium) according to US Patent 5 672 331 [19] starting from a mixture with molar composition: $0.065Na_2O{:}0.025Al_2O_3{:}SiO_2{:}0.1TPABr{:}15H_2O$. Based on the total weight of the synthesis mixture 40 ppm of colloidal silicalite seeds were added as a slurry. The mixture was heated in a stainless steel autoclave at 423 K for 72 h under static conditions.

ZSM-12 was synthesized according to Ref. [20] with some modifications. In a typical synthesis, 0.041 g of $NaAlO_2$ (technical grade, Riedel de Häen) was dissolved into 1.35 g of H_2O (Millipore water, resistivity >18 MΩ cm at 25 °C) and 5.15 g of tetraethylammonium hydroxide solution (TEAOH, 35 wt%, Sigma-Aldrich). To this solution, 10 g of colloidal silica was added (Ludox HS30, 30 wt% suspension in H_2O, Sigma-Aldrich), which resulted in a clear gel with a molar composition of 1.0 SiO_2:0.005 Al_2O_3:0.1225 TEA_2O:13.0 H_2O. The mixture was stirred at room temperature for 1 h, and then transferred into a teflon-lined steel autoclave with a full capacity volume of 50 ml (inner diameter of the teflon bottle of 34 mm and height of 55 mm). The autoclave was placed in an oven at 433 K for 5.5 days, and afterwards quenched with tap water. The precipitated product was washed with three batches of hot water (343–353 K). The powder product was obtained by filtration, and dried at 333 K overnight. The ZSM-12 sample has a Si/Al ratio of 105 and is referred to as ZSM-12-(105). A second ZSM-12 was prepared analogous to MTW-1, except that 0.071 g of $NaAlO_2$ was used resulting in a gel with molar composition of 1.0 SiO_2:0.0086 Al_2O_3:0.1225 TEA_2O:13.0 H_2O. This sample has a Si/Al ratio of 63 and is referred to as ZSM-12-(63).

Zeolite Beta was synthesized according to Ref. [21] with some modifications. In a typical synthesis, 2.40 g of silica (Sipernat 50, Evonik Degussa), 0.156 g of $Al(OH)_3$ (>63.5% Al_2O_3, Acros), and 0.592 g of NH_4F (>98%, Sigma-Aldrich) were added to 7.57 g of a tetraethylammonium hydroxide solution (TEAOH, 35 wt%, Sigma-Aldrich), which resulted in a gel with a molar composition of 1.0 SiO_2:0.025 Al_2O_3:0.225 TEA_2O:0.4 NH_4F:7.14 H_2O. The mixture was stirred at room temperature for 1 h, and then transferred into a teflon-lined steel autoclave with a full capacity volume of 50 ml (inner diameter of the teflon bottle of 34 mm and height of 55 mm). The autoclave was treated in a preheated oven at 443 K for 3 days, and afterwards quenched with tap water. The precipitated product was washed with three batches of hot water (343–353 K). The powder product was obtained by filtration, dried at 333 K overnight.

2.2. Alkaline treatment

Alkaline treatment was performed by adding 0.7 g of zeolite to 40 ml pre-heated alkaline solution (0.2, 0.5 or 1.0 M NaOH) (p.a., Merck) at 343 K, while stirring. This was followed by centrifugation (Eppendorf centrifuge 5804, 5000 rpm, 5 min), for zeolite Beta by ultra-centrifugation (Sorvall *RC5*$^+$ SS34 rotor, 18,000 rpm, 1 min) and decantation of the liquid followed by re-suspension with hot demineralized water. This procedure was repeated until the pH was 7 or less. The obtained sample will be referred to as zeolite-at[treatment time], after calcination (823 K, 3 h, 1 K min^{-1}) zeolite-at[treatment time]-cal is obtained.

To obtain the proton form of the zeolites, ion-exchange was performed in an aqueous 1 M NH_4NO_3 (p.a., Acros) solution at 353 K for 24 h, followed by filtering and washing. Per gram of zeolite 12 ml of ammonium nitrate solution was used. This procedure was repeated three times followed by calcination in air at 773 K for 3 h using a heating rate of 1 K min^{-1}. After the additional ion-exchange followed by calcination the obtained zeolite is referred to as H-zeolite-at[treatment time]-cal.

2.3. Structural characterization

Powder X-ray diffraction (XRD) patterns were obtained using a Bruker-Axs D8 series 2 with a $Co_{\alpha 1,2}$ source (λ = 0.179 nm). The porosity of the samples was studied using N_2 physisorption isotherms, which were recorded with a Micromeritics Tristar 3000 at 77 K. Prior to the physisorption measurements, the samples were dried overnight at 573 K in flowing nitrogen. The *t*-plot method [22] was applied to obtain the micro pore volume and the external surface area. Pore size distributions were obtained from the adsorption branch using the BJH-method [23]. The mesopore volume was calculated by integrating these plots from 2 to 50 nm. Ammonia temperature programmed desorption (TPD) was performed with a Micromeritics Autochem II. About ~150 mg of sample was dried at 573 K with a heating ramp of 5 K s^{-1} and kept there for 30 min after which the sample was cooled down to 473 K. After saturating the sample with ammonia, a 30 min dwell time was applied to obtain a stable baseline. Subsequently the temperature was increased to 923 K with a heating rate of 10 K s^{-1} and was kept there for 30 min. *n*-Hexane adsorption measurements were performed with a tapered element oscillating microbalance (TEOM) as described by Bitter et al. [24]. Morphology and crystal sizes were determined with a Tecnai FEI XL 30SFEG scanning electron microscope (SEM) at 15 kV and with a Tecnai 20 transmission electron microscope operated at 200 kV.

2.4. Catalysis

In a typical etherification reaction 0.05 mol of glycerol, 0.15 mol of 1-octene and 0.3 g of catalyst were loaded in a 100 ml stainless steel Parr autoclave. The autoclave was flushed with argon three times and then pressurized with argon to 10 bar. The autoclave was heated to 413 K and the solution was continuously mechanically stirred (750 rpm). The starting point of the reaction was taken when the autoclave reached the reaction temperature. After 3 h the reaction was stopped, the autoclave was cooled to 313 K and the reaction mixture was dissolved in a known amount of ethanol. The catalyst was separated by filtration, and a sample of the solution was taken for further analysis. More information about the procedure and analytical methods is described elsewhere [25]. Four ZSM-5 samples as well as four zeolite Beta samples were tested: H-ZSM-5-cal, H-ZSM-5-cal-at(0.2, 20), H-ZSM-5-cal-at(0.5, 20), H-ZSM-5-at(60)-cal, Beta-cal, Beta-at(15)-cal, Beta-at(120)-cal and H-Beta-at(120)-cal.

3. Results and discussion

Fig. 1 shows SEM images of three template containing zeolites: ZSM-5 (MFI), ZSM-12 (MTW) and zeolite Beta (BEA). All zeolites

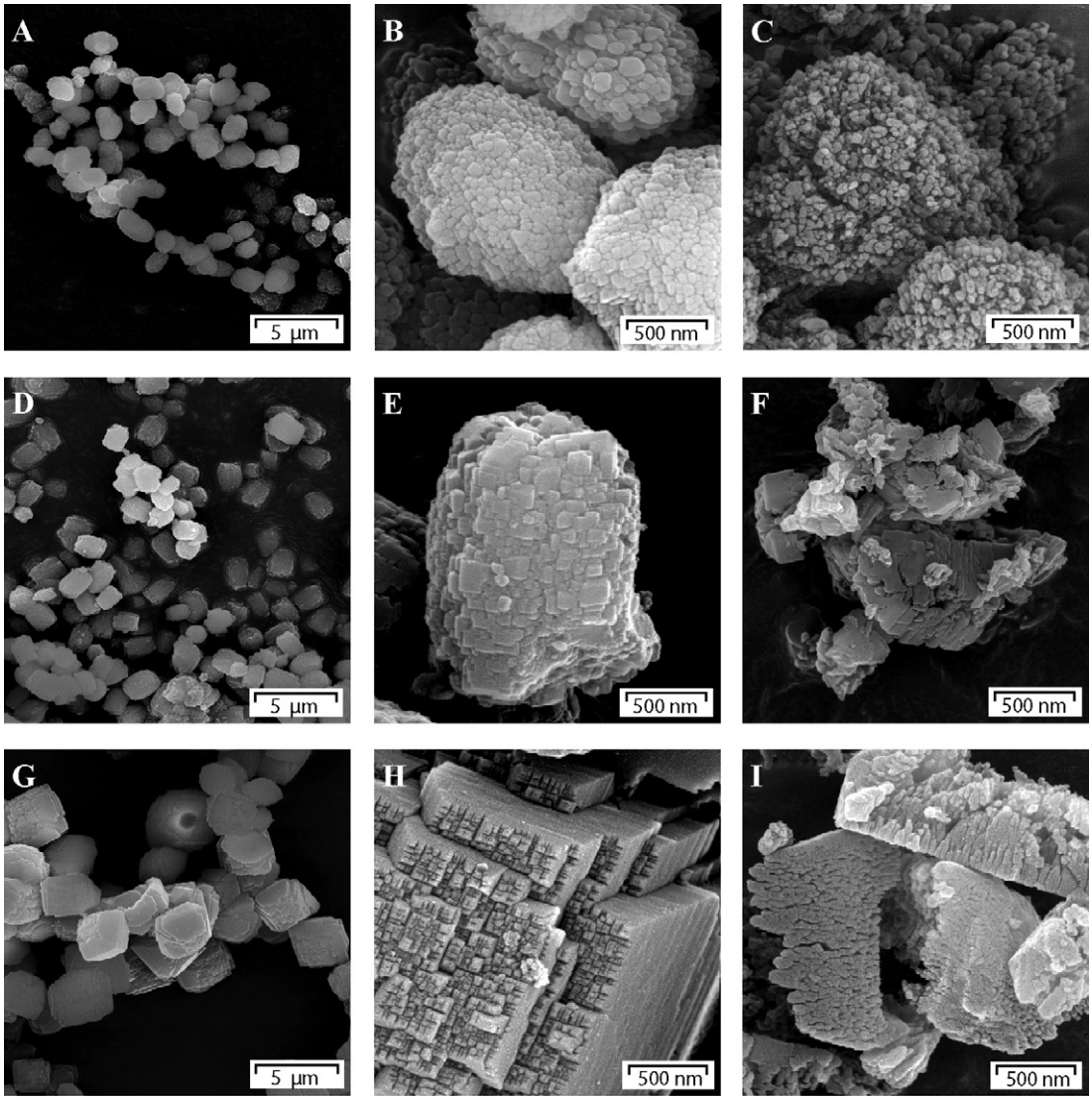

Fig. 1. SEM images of (A) ZSM-5-parent, (B) ZSM-5-parent, (C) ZSM-5-at(60), (D) ZSM-12-(105)-parent, (E) ZSM-12-(105)-parent, (F) ZSM-12-(105)-at(60), (G) Beta-parent, (H) Beta-parent, (I) Beta-at(120).

samples consist of small crystallites that have agglomerated into larger particles.

3.1. ZSM-5 (MFI)

The ZSM-5-parent had uniform particles with dimensions between 1 and 1.5 μm (Fig. 1A), that consisted of agglomerated nano-crystallites ranging from approximately 20 to 100 nm in size (Fig. 1B). The ZSM-5-parent displayed no micropore volume due to the presence of the TPA template and a low external surface area of 21 $m^2\ g^{-1}$ (Table 1). The mesopore volume is almost nil as a result of the dense packing of the crystallites. Upon calcination a micropore volume of 0.13 $cm^3\ g^{-1}$ was obtained while the external surface area (A_{ext}) had increased to 94 $m^2\ g^{-1}$. For direct comparison we will now first discuss the impact of alkaline treatment on template-free ZSM-5, and then the results for alkaline treatment on template-containing ZSM-5.

Alkaline treatment on template free ZSM-5 (after calcination) is described to be most effective for Si/Al ratios between 25 and 50 at/at with 0.2 M NaOH for 30 min [9,10]. Because of the small crystallites of the present ZSM-5 samples, a shorter treatment of 20 min in 0.2 M NaOH was performed. This resulted in the formation of a highly porous H-ZSM-5 sample with an external surface area of 205 $m^2\ g^{-1}$ (Table 1, Fig. 2). Alkaline treatment in 0.5 M NaOH solution for 20 min was performed resulting in an even higher external surface area of 233 $m^2\ g^{-1}$ (Table 1, Fig. 2). For both treatments the micropore volume was preserved. BJH analysis shows a predominant pore size of ~10 nm for the 0.2 M and ~20 nm for the 0.5 M NaOH treated samples. These results are close to the literature values described by Groen et al. [10] for which an external surface area of 235 $m^2\ g^{-1}$ and a predominant pore size of 10 nm are observed upon desilication of ZSM-5 zeolites. The initial Si/Al ratios (37–42 at/at) of the desilicated ZSM-5 zeolites are significantly higher compared to the Si/Al ratio (18 at/at) of the ZSM-5 zeolite used in this study. We hence confirmed that although desilication is a powerful tool to enhance accessibility, it is accompanied by a decrease in Si/Al ratio [8]. This implies that the acidity is changed, which can negatively affect catalysis [11–14].

A different approach to increase the accessibility of the ZSM-5 zeolite was performed by treating the parent ZSM-5 with the template still present, in alkaline solution of 1 M NaOH at 343 K for 20 to 60 min. Nitrogen physisorption (Fig. 3A) showed that alkaline treatment for 20 min resulted in an increased nitrogen uptake due to the formation of mesopores. A longer treatment time of 30

Table 1
Textural properties of ZSM-5 samples.

Sample code	V_{micro} [a] ($cm^3\ g^{-1}$)	A_{ext} [a] ($m^2\ g^{-1}$)	V_{meso} [b] ($cm^3\ g^{-1}$)	V_{total} [c] ($cm^3\ g^{-1}$)	Si/Al[d] (at/at)	*n*-Hexane uptake (wt.%)
ZSM-5-parent	–	21	0.04	0.05		
ZSM-5-cal	0.13	94	0.06	0.22		2.9
H-ZSM-5-cal	0.13	92	0.06	0.23	18	
Treated without template						
H-ZSM-5-cal-at(0.2, 20)	0.12	205	0.26	0.48	13	
H-ZSM-5-cal-at(0.5, 20)	0.12	233	0.49	0.80	9	
Treated with template						
ZSM-5-at(20)-cal	0.13	121	0.15	0.33	18	3.0
ZSM-5-at(30)	–	61	0.22	0.28		
ZSM-5-at(30)-cal	0.13	129	0.26	0.47		
ZSM-5-at(20)	–	52	0.12	0.15		
ZSM-5-at(60)	–	77	0.20	0.58		
ZSM-5-at(60)-cal	0.13	144	0.23	0.73		
H-ZSM-5-at(60)-cal	0.13	149	0.21	0.69	18	

[a] *t*-Plot method.
[b] BJH-method (adsorption branch).
[c] @ $p/p_o = 0.995$.
[d] ICP-AES.

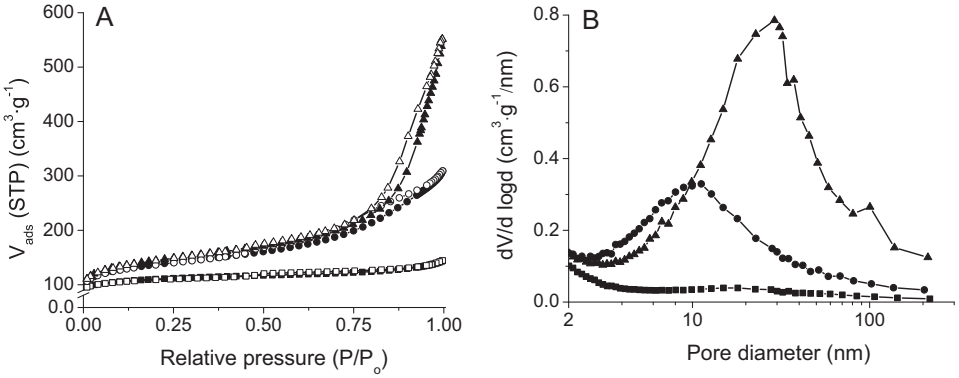

Fig. 2. N_2 adsorption (solid symbols) and desorption (open symbols) (A) and BJH desorption curves (B) of (■) ZSM-5-cal, (●) H-ZSM-5-cal-at(0.2, 20) and (▲) H-ZSM-5-cal-at(0.5, 20).

and 60 min shows an increased uptake of nitrogen that occurs at higher relative pressures indicating the formation of larger mesopores. From the BJH pore size distribution (Fig. 3B) we observe that mesopores of ~20 nm are present after 20 min of alkaline treatment that slowly grow with increased treatment time into large meso- and macro-pores with a predominant size of 30 and 60 nm. In Table 1 the textural properties of the samples are listed. A continual increase in the external surface area is observed from the 21 $m^2\ g^{-1}$ for the parent to 77 $m^2\ g^{-1}$ for ZSM-5-at(60). A likely explanation for these observations is that upon alkaline treatment small layers of the external surface area of the crystallites are dissolved, thereby increasing the mesoporosity of the agglomerates [26]. This hypothesis is further strengthened by the fact that neither the bulk Si/Al ratio (Si/Al = 18 at/at both before and after alkaline treatment) nor the crystallinity (Fig. 4) changed upon treatment. SEM (Fig. 1C) confirms that after alkaline treatment added mesoporosity is apparent between the crystallites within particles. If the ZSM-5 is calcined prior to the alkaline treatment in 1 M NaOH complete dissolution occurred within min. After calcination all ZSM-5 samples show, whether alkaline treated or not, a similar micropore

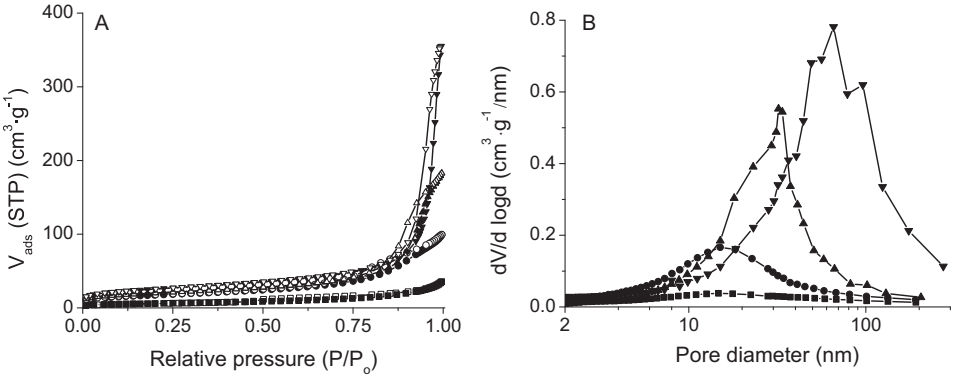

Fig. 3. N_2 adsorption (solid symbols) and desorption (open symbols) (A) and BJH desorption curves (B) of (■) ZSM-5-parent, (●) ZSM-5-at(20) (▲) ZSM-5-at(30) (▼) ZSM-5-at(60).

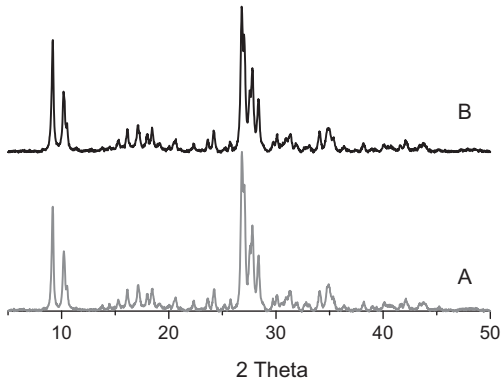

Fig. 4. XRD pattern of ZSM-5-parent (A) and ZSM-5-at(60) (B).

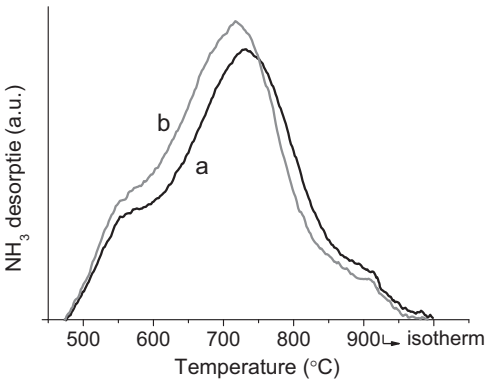

Fig. 5. Ammonia TPD curves of H-ZSM-5-cal (a) and H-ZSM-5-at(60)-cal (b).

volume (Table 1). The mesoporosity is unaffected by the calcination step (Fig. S1). *n*-Hexane uptake measurements indicated that the micropores are fully accessible also for large molecules with similar values as those described in literature (Table 1, Fig. S2) [24]. NH_3 TPD measurements were performed on the proton form of the ZSM-5 to probe the acid sites. Similar curves for parent and alkaline treated ZSM-5 indicate that the acid sites are completely preserved (Fig. 5). A slight shift is observed towards lower temperatures, which could be the result of faster transport of NH_3 [27] because of the added mesoporosity.

Comparing the alkaline treatment with and without template, we can conclude that without a template a significantly larger increase in external surface area is obtained. A second advantage is that the combination of intra- and inter-crystalline mesopores provides an effective reduction of the pathlength towards the active sites [13]. However, the Si/Al ratio decreases, and hence the strength of the acid sites. Although alkaline treatment on template-containing samples gives a more modest increase in surface area, this is obtained without altering the acid site strength. Hence alkaline treatment in the presence of a template might provide a very useful strategy if extra mesoporosity is desirable, but the properties of the acid sites, such as for instance reflected in the selectivity when used as a catalyst, should not be affected.

3.2. ZSM-12 (MTW)

ZSM-12 samples were synthesized in two different gel compositions resulting in two samples ZSM-12-(105) and ZSM-12-(63) with Si/Al ratios of 105 and 63, respectively. The morphology of the two samples was very similar, consisting of agglomerates (1 μm × 2 μm, Fig. 1D) that contained small crystallites ranging in size from approximately 50 to 200 nm (Fig. 1E).

Alkaline treatment was performed in 1 M NaOH at 343 K on the non-calcined ZSM-12 samples (Table 2). Only minor differences between the two samples are observed. The mesopore formation after 30 min is slightly higher for the aluminum poor ZSM-12-(105) (0.15 $cm^3\,g^{-1}$) compared to the more aluminum rich ZSM-12-(63) (0.10 $cm^3\,g^{-1}$). This is in agreement with Wei and Smirniotis [18] who observed a slightly faster rate of desilication for higher Si/Al ratio, although this could not be proven due to the presence of different amounts of template. After treatment for 60 min we observed a decrease in both mesopore volume and external surface area, and the formation of large meso- and macro-pores (Fig. S3). SEM images (Fig. 1F) show that the agglomerates have fallen apart into various sized smaller agglomerates. The small differences between the two samples suggest that there is a minor influence of the aluminum content on alkaline treatment, and that the alkaline treatment is primarily controlled by the presence of the template.

Our results show that alkaline treatment in 1 M NaOH at 343 K enhances the mesoporosity when applied to different commercially available zeolites. The results on the low aluminum content ZSM-12 demonstrate that mesoporosity can be introduced by alkaline treatment in the presence of a template, regardless of the Si/Al ratio, whereas without a template present this is limited to a upper Si/Al ratio of ~50 (at/at) [9]. The differences that exist between the tested samples seem to be the result of the particle/crystallite size of the parent material.

3.3. Beta (BEA)

The morphology of the synthesized zeolite Beta (Fig. 1G) was slightly different from the other two zeolites. No individual crystallites were observed, but instead large truncated bipyramidal crystals with smooth surfaces and a width of 5 μm. Higher magnification reveals that the top of the crystallites is covered with small extrusions between 20 and 30 nm in size (Fig. 1H).

Table 2
Textural properties of ZSM-12 samples.

Sample code	V_{micro}[a] ($cm^3\,g^{-1}$)	A_{ext}[a] ($m^2\,g^{-1}$)	V_{meso}[b] ($cm^3\,g^{-1}$)	V_{total}[c] ($cm^3\,g^{-1}$)	Si/Al[d] (at/at)
ZSM-12-(105)	–	1	–	0.01	105
ZSM-12-(105)-at(15)	–	36	0.05	0.06	–
ZSM-12-(105)-at(30)	–	47	0.15	0.24	–
ZSM-12-(105)-at(60)	–	39	0.07	0.26	99
ZSM-12-(63)	–	2	–	0.01	63
ZSM-12-(63)-at(15)	–	42	0.05	0.06	–
ZSM-12-(63)-at(30)	–	46	0.11	0.13	–
ZSM-12-(63)-at(60)	–	44	0.07	0.27	60

[a] *t*-Plot method.
[b] BJH-method (adsorption branch).
[c] @ $p/p_o = 0.995$.
[d] ICP-AES.

Table 3
Textural properties of zeolite Beta samples.

	V_{micro}[a] ($cm^3\ g^{-1}$)	A_{ext}[a] ($m^2\ g^{-1}$)	V_{meso}[b] ($cm^3\ g^{-1}$)	V_{total}[c] ($cm^3\ g^{-1}$)	Si/Al[d] (at/at)
Beta-cal	0.23	77	0.03	0.29	17
Beta-at(15)-cal	0.21	181	0.09	0.35	–
Beta-at(120)-cal	0.21	164	0.34	0.73	16
H-Beta-at(120)-cal	0.20	158	0.29	0.54	–
Zeolyst-CP 814E-cal	0.17	227	0.36	0.83	12.5

[a] *t*-Plot method.
[b] BJH-method (adsorption branch).
[c] @ $p/p_o = 0.995$.
[d] ICP-AES

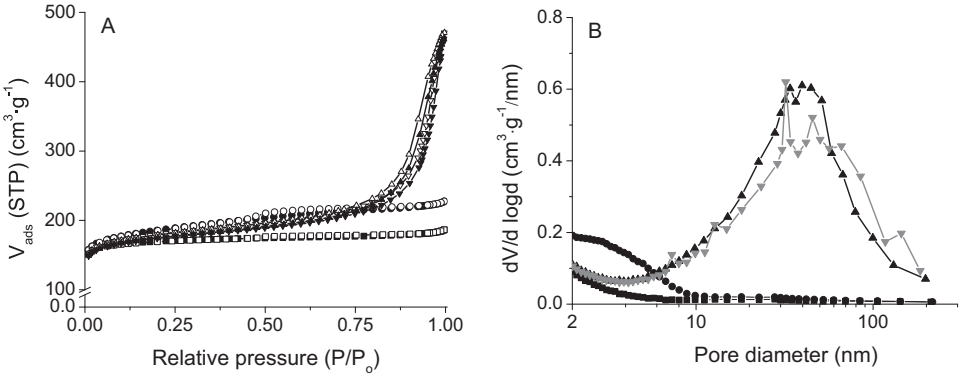

Fig. 6. N_2 adsorption (solid symbols) and desorption (open symbols) (A) and BJH desorption curves (B) of (■) Beta-cal, (●) Beta-at(15)-cal, (▲) Beta-at(120)-cal and (▼) H-Beta-at(120)-cal.

Alkaline treatment in 1 M NaOH for 15 min on the template containing zeolite Beta followed by calcination resulted in an increase in external surface from 70 to 181 $m^2\ g^{-1}$ and similar micropore volume (Table 3, Fig. 6). The BJH pore size distribution (Fig. 6B) shows that upon alkaline treatment for 15 min small mesopores between 2 and 10 nm have formed. Another alkaline treatment was performed for 120 min, which resulted in a slightly lower external surface area of 164 $m^2\ g^{-1}$ compared to the 15 min treatment. This sample has large mesopores of ~40 nm (Fig. 6B) and SEM images (Fig. 1) show that some of the particles have fallen apart into smaller fragments, similar to what is observed for the ZSM-12 sample after 60 min of treatment. To prevent the loss of small clusters of zeolite Beta all washing steps were followed by ultra-centrifugation, from which clear fluids were decanted. The smaller agglomerate fractions allowed the use TEM to look at the crystallites (Fig. 7). The interior of zeolite Beta consisted of smaller crystallites that are aligned parallel with inter-crystalline porosity.

No sodium was present during synthesis, hence calcination resulted in the proton form of zeolite Beta. NH_3 TPD measurements were performed to measure if the alkaline treatment affects the acidity. For the Beta-parent two peaks (Fig. 8a) were observed, the first peak at ~475 K is ascribed to weak Lewis acid sites, and the second peak at ~670 K [28] to Brønsted acid sites [29]. For comparison a commercially available zeolite Beta from Zeolyst was analyzed (Fig. 8d). A similar pattern was observed with slightly more Brønsted acid sites. This is a direct result of the lower Si/Al ratio (12.5 at/at) and confirmed the assignment of the peak. For the Zeolyst material a third peak or shoulder is observed at ~780 K, which could be the result of strong Lewis acid sites. Compared to the parent no change for the weak Lewis acidity (~475) was observed after 15 min of alkaline treatment (Fig. 8e). The Brønsted acidity (~670 K) is slightly lower compared to the parent and deconvolution revealed a fourth peak at 570 K. This peaks might be the result of NH_3 adsorption on Na^+ sites, which is a weaker than NH_3 adsorption on H^+ sites and desorption therefore occurs at lower temperatures [30]. After 120 min of alkaline treatment a similar pattern as for 15 min was observed although the peak at ~780 K is slightly increased (Fig. 8b). The percentage NH_3

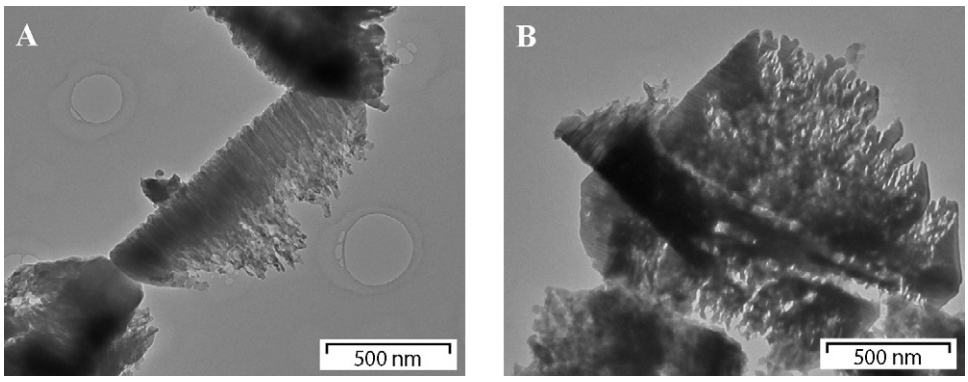

Fig. 7. TEM images of Beta-at(120).

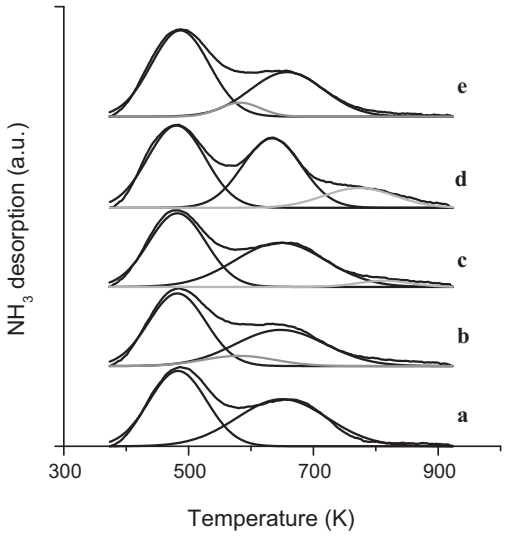

Fig. 8. Ammonia TPD curves of Beta-parent (a), Beta-at(120)-cal (b), H-Beta-at(120)-cal (c), Zeolyst Cp814N (d) and Beta-at(15)-cal (e).

adsorbed onto Na^+ ions is approximately between 15% and 20% of the total cationic sites of the zeolite. Upon ion exchange and calcination of the Beta-at(120)-cal sample the Na^+ peak at 570 K disappears (Fig. 8c), thereby restoring Brønsted acidity. Clearly during alkaline treatment some cationic sites are ion-exchanged with sodium. Presumably this ion-exchange occurs close to the external surface area as the template is still present inside the micropores after ion exchange. This implicates that an additional ion exchange/calcination step is necessary to obtain a fully active catalyst.

3.4. Catalysis

We have sofar seen that the porosity can be increased with alkaline treatment without changing the acidity (or bulk Si/Al ratio). It is hence interesting to test if the catalytic performance is enhanced. The influence of the alkaline treatment on the catalytic properties of Beta and ZSM-5 zeolites was investigated in the etherification of 1,2-propylene glycol with 1-octene (Scheme 1). The direct etherification of biomass-based glycols was recently reported to take place with high activity and selectivity over the H-Beta zeolites [25,31,32]. Furthermore, the etherification activity of the H-Beta zeolites was correlated to both the crystal size and the external surface area of the zeolite, while ZSM-5 was found to be less active and selective [25,31,32], where most probably the reaction takes place as observed by confocal fluorescence microscopy [32]. Therefore, the etherification of 1,2-propylene glycol with 1-octene can be used as a test reaction for the effect of the alkaline treatment on the catalytic activity of the zeolites. The tests were performed at low conversions of the alcohol substrate in order to be able to relate catalytic activity of the zeolite with the pretreatment process. The results of the etherification of 1,2-propylene glycol with 1-octene are presented in Table 3 and are compared to a commercial Beta and ZSM-5 zeolites (Zeolyst-*CP 814E)*, with smaller particle size which previously showed a very high activity for this reaction [25,31].

Table 4
Etherification of 1,2-propylene glycol with 1-octene over ZSM-5 and Beta zeolites.

Catalyst	Conv. (%)	$Sel._{C8\text{-}ether}$ (%)	$Sel._{C16\text{-}ether}$ (%)	$Sel._{other}$ (%)
H-ZSM-5-cal	1.2	95	0	5
H-ZSM-5-cal-at(0.2, 20)	5.0	98	1	2
H-ZSM-5-cal-at(0.5, 20)	3.8	96	2	2
H-ZSM-5-at(60)-cal	5.6	98	1	1
Beta-cal	33	88	3	9
Beta-at(15)-cal	26	91	4	5
Beta-at(120)-cal	23	91	4	5
H-Beta-at(120)-cal	40	88	5	7
Zeolyst-CP814N	45	90	4	6

Reaction conditions: 0.3 g catalyst, 0.05 mol 1,2-propylene, 0.15 mol 1-octene, 413 K, 3 h, 10 bar Ar.

The etherification of 1,2-propylene glycol with 1-octene over all H-ZSM-5 and H-Beta zeolites produced with high selectivity octyl-ether (Table 4). Side products were small amounts of di-ether (C16), and dehydrated and cyclic derivatives of 1,2-propylene glycol, consistent with previously reported results [25,31]. The untreated H-ZSM-5-cal has a low conversion (1.2%) similar to values obtained in literature [25]. The selectivity is with 95% towards the mono-isomer (Table 4) significantly better than the values described in literature (<82% after 5 h of reaction) [25]. The alkaline treated H-ZSM-5-cal-at(0.2, 20) showed a fourfold increase in conversion (5.0%) as well as a slightly better selectivity. The alkaline treatment on the template containing ZSM-5 (H-ZSM-5-at(60)-cal) resulted in the best catalytic performance with a conversion of 5.6% and a selectivity of 98%. This is at first sight unexpected, as the porosity of the H-ZSM-5-at(60)-cal is considerably lower than that of H-ZSM-5-cal-at(0.2/0.5, 20) (149 vs. 205 and 233 $m^2\ g^{-1}$). A plausible explanation is that the pore entrances of the H-ZSM-5-cal-at(0.2/0.5, 20) samples are partly obstructed by extra framework aluminum [14].

Prior to testing, the parent and alkaline treated zeolite Beta samples (Table 3) were calcined to obtain the proton form. One sample,

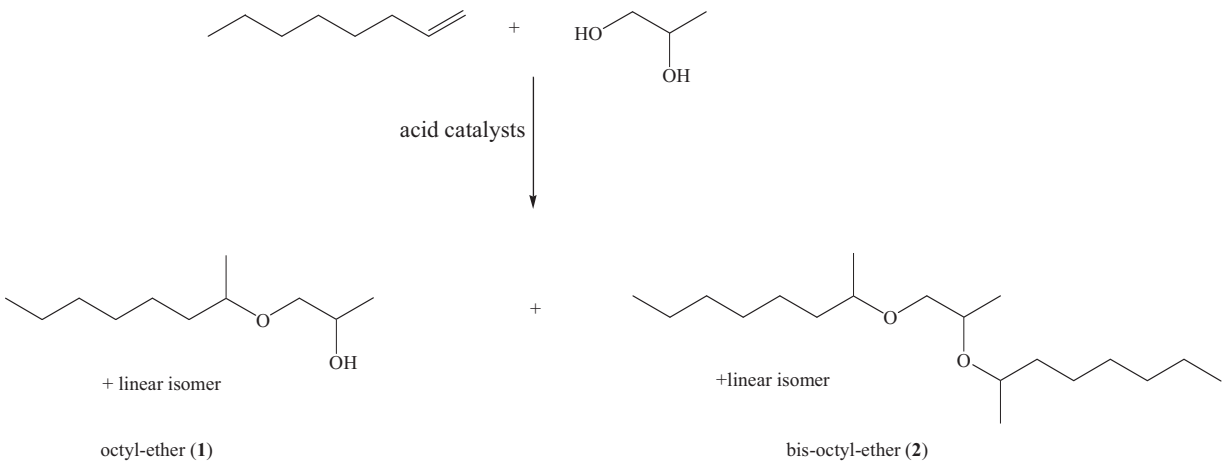

Scheme 1. Etherification of 1,2-propylene glycol with 1-octene.

H-Beta-at(120)-cal, received an NH_4-ion exchange in 1 M NH_4NO_3 followed by calcination in air. The etherification of 1,2-propylene glycol with 1-octene over all H-Beta zeolites produced mainly the octyl-ethers with selectivities over 88% (Table 4). The mono-ether (C8-ether) was obtained for all the catalysts as the main reaction product and the side products mostly consists of small amounts of dehydrated and cyclic derivatives of 1,2-propylene glycol, consistent with other results [25,31]. The most active catalyst was the commercial zeolite, with a ratio of Si/Al of 12.5 and with the highest external surface (Table 3). With this catalyst a conversion of 1,2-propylene glycol of 45% was observed after 3 h of reaction. The in-house synthesized Beta-cal (initial particle size of about ~2 μm) presented lower conversions, but a similar product distribution and selectivity was found as for the commercial zeolite. The higher external surface area of the alkaline treated zeolite Beta samples was expected to result in an increased conversion for this reaction. However, a short alkaline treatment of just 15 min was found to result in a decrease of the alcohol conversion from 33% to 26% (Table 4). This is despite the increase in external surface of 72–185 $m^2\,g^{-1}$ upon alkaline treatment. A longer alkaline treatment of 120 min (Beta-at(120)-cal) resulted in an even lower conversion of 23%. The selectivity towards the C8-ether increased slightly from 88% to 91%, while the selectivity of the by-products decreased from 9% to 5%. The decreased conversion can be attributed to the presence of Na^+ ions that remained after alkaline treatment (Fig. 8B). As discussed in Section 3.4 the Na^+ ions are expected to be located near the external surface area as the interior of the zeolite and thus the acid sites were protected from alkaline treatment by the template. After removal of the Na^+ ions upon ion exchange with NH_4NO_3 followed by calcination (H-Beta-at(120)-cal) the conversion almost doubled from 23% to 40%. This conversion is also significantly higher than the parent Beta (33% conversion), which is expected given the higher external surface area 77 vs. 158 $m^2\,g^{-1}$.

The strong increase in conversion for higher external surface areas suggests that the etherification of 1,2-propylene glycol with 1-octene is affected by intra-crystalline diffusion, as suggested earlier [25,31]. An important factor are the pore systems of the zeolites. Comparing samples with similar Si/Al atomic ratio (~17 at/at) and surface area (~155 $m^2\,g^{-1}$), zeolite Beta is much more active and not as prone to pore blocking as ZSM-5. This is explained by their different pore geometries, with a 10-ring (5.1 × 5.5 Å) for ZSM-5 and a 12-ring channel (7.1 × 7.3 Å) for zeolite Beta. Most importantly, we can conclude that in both cases alkaline treatment of template containing zeolites results in added porosity and enhanced catalytic activity, while selectivity is unaffected or even improved.

4. Conclusions

Template containing ZSM-5 (Si/Al ratio 18 at/at) was subjected to alkaline treatment in 1 M NaOH at 343 K to induce extra mesoporosity. The ZSM-5 samples consisted of small crystallites between 20 and 100 nm in size that were agglomerated into larger particles of ~1 μm. After alkaline treatment for 60 min the external surface area was increased from 21 to 77 $m^2\,g^{-1}$. Because of the presence of the template the micropores were unaffected by the alkaline treatment and after calcination the full micropore volume was obtained, while the added mesoporosity was preserved. Alkaline treatment without the template present resulted in higher external surface areas, but also in a decrease in Si/Al ratio to 13 (0.2 M NaOH) and 8 (0.5 M NaOH). SEM showed that the nature of the mesoporosity was inter-crystalline and intra-particle. Additional experiments on ZSM-12 gave similar results and showed that the treatment can be applied to a range of zeolites regardless of the Si/Al ratio. It was also determined that the morphology of the parent zeolite, i.e. crystallite/particle size, determines the amount of added mesoporosity in which smaller crystallites give rise to higher porosities. Alkaline treatment on sodium-free zeolite Beta for 120 min led to an increase in the external surface from 77 to 164 $m^2\,g^{-1}$. As a result the large Beta particles (5 μm) showed de-agglomeration, which made it possible to study the individual crystallites by TEM. NH_3-TPD measurements showed that after alkaline treatment 15–20% of the total protonic sites were ion exchanged with sodium cations. The sodium cations were probably located near the external surface area, as the interior of the crystallites is protected by the templates molecules. Subsequent ion exchange/calcination was performed to convert the zeolite fully into the proton form. As a showcase reaction the catalytic performance of alkaline treated ZSM-5 and zeolite Beta were tested for the etherification of 1,2-propylene glycol with 1-octene. This reaction was previously [25,31,32] expected to be a surface catalyzed reaction. A 1% conversion of 1,2-propylene glycol for the ZSM-5-parent was measured. Upon alkaline treatment on template containing ZSM-5 the conversion increased to 5.6% and selectivity increased from 95% to 98%. Conversion of 1,2-propylene glycol for the alkaline treated ZSM-5 zeolite was with 5.0% and 3.8% lower than with a template despite a higher external surface area. For zeolite Beta significantly higher conversions were measured although upon alkaline treatment initially a decrease in conversion (33–23%) was observed despite the higher porosity. However, after the NH_4-ion exchange/calcination the conversion increased to 40%, in line with the previous studies. The presence of the sodium cations near the external surface apparently inhibited the reaction, which makes it likely that the etherification of 1,2-propylene glycol with 1-octene over zeolite Beta is affected by intra-crystalline diffusion.

During alkaline treatment of templated zeolites silicon as well aluminum species are slowly dissolved. This process created smaller crystallites and inter-crystalline mesoporosity. The presence of the template inside the micropores assures that the acid sites are not affected by the treatment. The increase in porosity leads to enhanced catalytic performance, and provides an opportunity to decouple the acidity from accessibility of zeolites, and can be used to optimize and gain insight in zeolite catalysis.

Acknowledgements

The authors thank Dr. M. Mertens and Dr. M.J. Janssen (ExxonMobil, Belgium) for supplying the ZSM-5 sample. J. Zečević for TEM, M. Versluijs-Helder for SEM, V. Koot for NH_3-TPD and ACTS-ASPECT for financial support.

Appendix A. Supplementary data

Supplementary data associated with this article can be found, in the online version, at doi:10.1016/j.cattod.2010.10.101.

References

[1] R.M. Barrer, P.J. Denny, J. Chem. Soc. (1961) 971–982.
[2] R.M. Barrer, L.W.R. Dicks, J. Chem. Soc. A (1967) 1523–1529.
[3] G.T. Kerr, US Patent 3.247.195, 1966.
[4] R.M. Barrer, P.J. Denny, E.M. Flanigane, US Patent 3.306.922, 1967.
[5] C Bearlocher, L.B McCusker, D.H. Olsen, Atlas of zeolite framework types, 2007.
[6] S. van Donk, A.H. Janssen, J.H. Bitter, K.P. de Jong, Catal. Rev. Sci. Eng. 45 (2003) 297–319.
[7] M. Ogura, S. Shinomiya, J. Tateno, Y. Nara, E. Kikuchi, M. Matsukata, Chem. Lett. 29 (2000) 882.
[8] M. Ogura, S. Shinomiya, J. Tateno, Y. Nara, M. Nomura, E. Kikuchi, M. Matsukata, Appl. Catal. A 219 (2001) 33–43.
[9] J.C. Groen, J.C. Jansen, J.A. Moulijn, J. Pérez-Ramirez, J. Phys. Chem. B 108 (2004) 13062–13065.
[10] J.C. Groen, L.A.A. Peffer, J.A. Moulijn, J. Pérez-Ramírez, Chem. Eur. J. 11 (2005) 4983–4994.

[11] J.C. Groen, S. Abelló, L.A. Villaescusa, J. Pérez-Ramírez, Microporous Mesoporous Mater. 114 (2008) 93–102.
[12] M.S. Holm, S. Svelle, F. Joensen, P. Beato, C.H. Christensen, S. Bordiga, M. Bjørgen, Appl. Catal. A 356 (2009) 23–30.
[13] J.C. Groen, T. Bach, U. Ziese, A.M. Paulaime-van Donk, K.P. de Jong, J.A. Moulijn, J. Pérez-Ramírez, J. Am. Chem. Soc. 127 (2005) 10792–10793.
[14] C. Fernandez, I. Stan, J.P. Gilson, K. Thomas, A. Vicente, A. Bonilla, J. Pérez-Ramírez, Chem. Eur. J. 16 (2010) 6224–6233.
[15] J. Pérez-Ramírez, S. Abelló, A. Bonilla, J.C. Groen, Adv. Funct. Mater. 19 (2009) 164–172.
[16] J. Pérez-Ramírez, D. Verboekend, A. Bonilla, S. Abelló, Adv. Funct. Mater. 19 (2009) 3972–3979.
[17] M.S. Holm, M.K. Hansen, C.H. Christensen, Eur. J. Inorg. Chem. (2009) 1194–1198.
[18] X. Wei, P.G. Smirniotis, Microporous Mesoporous Mater. 97 (2006) 97–106.
[19] J.P. Verduijn, US Patent 5 672 331, Exxon Chemical Patents Inc., United States, 1997.
[20] S. Gopal, K. Yoo, P.G. Smirniotis, Microporous Mesoporous Mater. 49 (2001) 149–156.
[21] B.W. Lu, H. Jon, T. Kanai, Y. Oumi, K. Itabashi, T. Sano, J. Mater. Sci. 41 (2006) 1861–1864.
[22] B.C. Lippens, J.H. de Boer, J. Catal. 4 (1965) 319–323.
[23] E.P. Barrett, L.G. Joyner, P.P. Halenda, J. Am. Chem. Soc. 73 (1951) 373–380.
[24] J.H. Bitter, A.A. Battiston, S. van Donk, K.P. de Jong, D.C. Koningsberger, Microporous Mesoporous Mater. 64 (2003) 175–184.
[25] A.M. Ruppert, A.N. Parvulescu, M. Arias, P.J.C. Hausoul, P.C.A. Bruijnincx, R.J.M. Klein Gebbink, B.M. Weckhuysen, J. Catal. 268 (2009) 251–259.
[26] A.N.C. van Laak, R.W. Gosselink, S.L. Sagala, J.D. Meeldijk, P.E. de Jongh, K.P. de Jong, Appl. Catal. A: Gen. 382 (2010) 65–72.
[27] F. Lónyi, J. Valyon, Microporous Mesoporous Mater. 47 (2001) 293–301.
[28] Y. Miyamoto, N. Katada, M. Niwa, Microporous Mesoporous Mater. 40 (2000) 271–281.
[29] A.M. Camiloti, S.L. Jahn, N.D. Velasco, L.F. Moura, D. Cardoso, Appl. Catal. A: Gen. 182 (1999) 107–113.
[30] C. Costa, J.M. Lopes, F. Lemos, F.R. Ribeiro, J. Mol. Catal. A: Chem. 144 (1999) 221–231.
[31] A.N. Parvulescu, P.J.C. Hausoul, P.C.A. Bruijnincx, R.J.M. KleinGebbink, B.M. Weckhuysen, Catal. Today 158 (2010) 130–138.
[32] A.N. Parvulescu, D. Mores, E. Stavitski, C.M. Teodorescu, P.C.A. Bruijnincx, R.J.M.K. Gebbink, B.M. Weckhuysen, J. Am. Chem. Soc. 132 (2010) 10429–10439.